

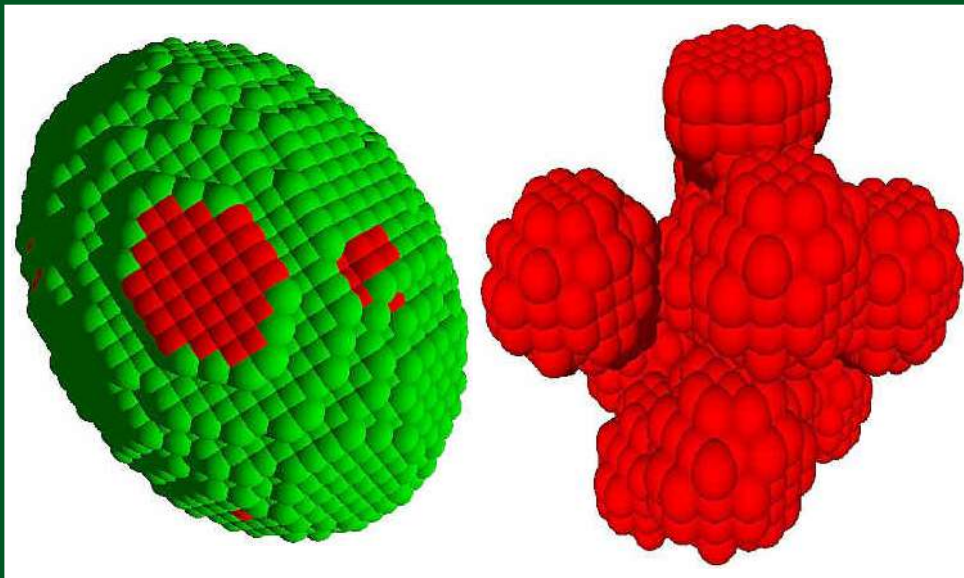
AJP

ISSN : 0971 - 3093

Vol 24, No 8, August, 2015

ASIAN JOURNAL OF PHYSICS

An International Research Journal



ANITA PUBLICATIONS

FF-43, 1st Floor, Mangal Bazar, Laxmi Nagar, Delhi-110 092, India
B O : 2, Pasha Court, Williamsville, New York-14221-1776, USA



FUSE view of interstellar O VI

Rathin Sarma¹, Amit Pathak² and J K Sarma²

¹Department of Physics, Hojai College, Hojai-782 435, India

²Department of Physics, Tezpur University, Tezpur-784 028, India

Far-Ultraviolet Spectroscopic Explorer (FUSE) telescope has played an important role in the study of interstellar OVI. Here we present a brief review of the distribution and some of the properties of O VI in the Milky Way (MW) and in the nearby galaxies; the Large Magellanic Cloud (LMC) and the Small Magellanic Cloud (SMC) as found by different FUSE observations. The distribution of O VI throughout the Galaxy and in the LMC and the SMC is patchy. O VI column density has been found to vary on a very small scale. There are variations in the O VI content of the northern hemisphere compared to the southern hemisphere of the Milky Way. Surprisingly, despite being of lower metallicity, the O VI column density in the SMC has been found to be higher compared to the Milky Way and the LMC. © Anita Publications. All rights reserved.

Keywords: Far-Ultraviolet Spectroscopic Explorer (FUSE), Milky Way (MW), Large Magellanic Cloud (LMC), Small Magellanic Cloud (SMC).

1 Introduction

Hot gases ($\sim 10^5 - 10^6$ K) are important constituents of the interstellar medium (ISM). The existence of hot gas in the Milky Way halo was first proposed by Spitzer [1]. The absorption lines in the UV spectra of lithium like ions C IV, N V and O VI reveal fundamental information about the hot gas. Among these ions, O VI, which has strong resonance doublet at 1032 and 1037 Å, is an important tool to study the warm-hot phase of the ISM. Other than hydrogen and helium, oxygen is the most abundant element with large oscillator strengths for O VI lines ($f_{\lambda 1032} = 0.133$ and $f_{\lambda 1037} = 0.067$) [2]. The ionization of O V to O VI needs 113.9 eV which requires very high energy photons for OVI production via photoionization in the ISM. Alternate and a well accepted mechanism is that the OVI ions form from collisional ionization in the hot gas ($T > 2 \times 10^5$ K). In collisional ionization equilibrium (CIE) the maximum number density of OVI corresponds to a temperature of 2.8×10^5 K with ionization fraction $n(\text{OVI})/n(\text{O}) = 0.22$ [3].

OVI was first studied by the *Copernicus* satellite with the high-resolution far-UV spectrometer [4, 5]. In another survey of O VI towards 72 stars using *Copernicus* observations, Jenkins confirmed the existence of hot gas in the ISM [6,7]. *Copernicus* observations were limited to stars brighter than $V \sim 7.0$. The *International Ultraviolet Explorer* (IUE) and the *Hubble Space Telescope* (HST) were able to observe C IV, N V, and Si IV only. The *Hopkins Ultraviolet Telescope* (HUT) [8] and the spectrograph on-board the *Orbiting and Retrievable Far and Extreme Ultraviolet Spectrometer* (ORFEUS) [9] observed OVI for a few lines of sight.

2 The FUSE Observatory

The *FUSE* satellite, which was launched in 1999, provides much better scope to study O VI in the ISM. The spacecraft and the scientific mission of *FUSE* have been described in detail by Moos *et al* [10] and Sahnou *et al* [11]. This satellite provides an opportunity to study several essential aspects of astrophysics, mainly the resonance doublet of O VI that traces interstellar gas in the warm-hot regime, the ground state electronic transitions of H₂, Deuterium transitions short-ward of Lyman alpha, etc.

Corresponding author :

e-mail: amitpah@gmail.com (Amit Pathak)

FUSE covers the far-ultraviolet wavelength range 905-1187 Å that includes the O VI doublet wavelengths for the Milky Way and nearby galaxies and the nearby intergalactic medium. The other features that make *FUSE* an ideal instrument to study O VI are its excellent resolution (20 km s^{-1}), large effective area ($20 - 70 \text{ cm}^2$) and high radiometric efficiency.

The optical arrangement in *FUSE* is based on a Rowland circle design having four optical channels. Each channel consists of a mirror, a focal plane assembly (FPA), a diffraction grating and part of a detector. Two mirrors and gratings are coated with lithium fluoride (LiF) over a layer of aluminum. The other two mirrors and gratings are coated with silicon carbide (SiC). The SiC channels cover the wavelength range 905 – 1104 Å, while the LiF channels cover the 990 – 1185 Å band. The spectra from the four channels are imaged onto two photon counting micro channel plate (MCP) detectors, each divided into two individual segments (A and B). Light from the two channels fall on each of the detectors resulting in eight ~ 90 Å individual spectra. These are identified according to the segments: LiF 1A, LiF 2A, LiF 1B, LiF 2B, SiC 1A, SiC 2A, SiC 1B and SiC 2B. [Figure 1](#) shows the 1A detector segment raw image for a typical *FUSE* observation.

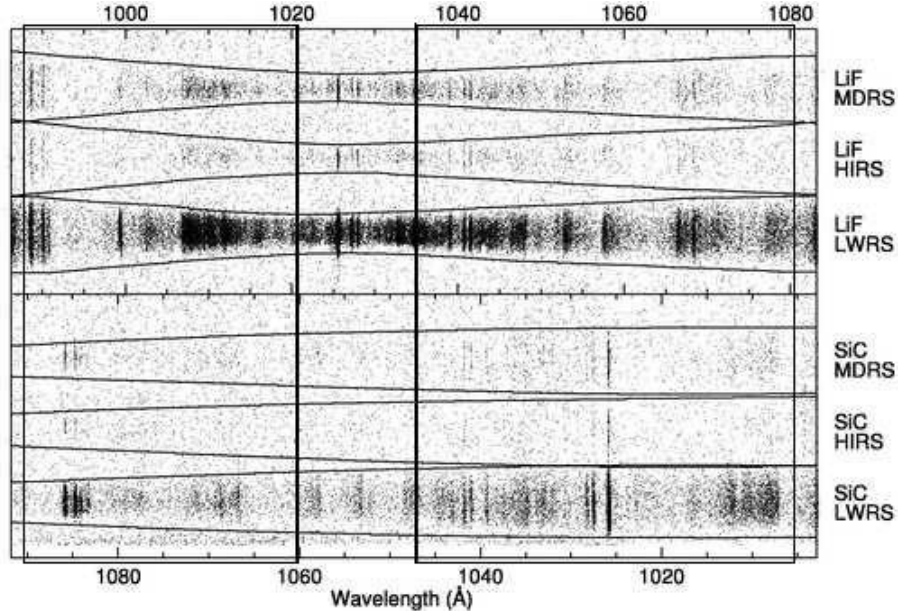


[Fig 1.](#) FUSE 1A detector segment for a typical observation. [12]

There are four apertures for simultaneous observations in *FUSE*. The LWRS is the most frequently used aperture with size $(30 \times 30) \text{ arcsec}^2$. MDRS is a medium-resolution aperture having size $(4 \times 20) \text{ arcsec}^2$. With aperture size $(1.25 \times 20) \text{ arcsec}^2$, HIRS gives the highest resolution. A pinhole aperture PINH with size approximately 0.5 arcsec^2 in diameter also exists but has never been used on orbit.

During its operation period (1999 – 2007), *FUSE* produced high resolution data that includes OVI absorption lines produced in the warm – hot interstellar gas of the Milky Way towards Galactic and extragalactic objects. All the public and proprietary *FUSE* data is stored at the Multi-mission Archive at the Space Telescope Science Institute (MAST) and are freely available for download. The *FUSE* data available at MAST is reduced with the CalFUSE [\[13\]](#) software package.

The *FUSE* Science Team designed programs to investigate OVI distribution in the ISM of the Milky Way. Galactic OVI studies have been concentrated on the Galactic disk, and the Galactic halo.

2.1 The apparent optical depth (AOD) method

The apparent optical depth (AOD) technique [14-16] has been widely used to measure the equivalent width and column density of the O VI line absorption. This method uses an AOD (τ_a) in terms of velocity defined as,

$$\tau_a(v) = \ln[I_0(v)/I_{\text{obs}}(v)],$$

where I_0 is the continuum intensity, I_{obs} is the absorption line intensity in terms of velocity. If the FWHM of the absorption line is completely resolved, the apparent optical depth is a reliable approximation of the true optical depth. *FUSE* with its high resolution spectrograph is able to completely resolve the O VI doublet. The apparent column density ($N_a(v)$ [atoms $\text{cm}^{-2} \text{km s}^{-1}$]) is calculated by the relation

$$N_a(v) = m_e c \tau_a(v) / \pi e^2 f \lambda = 3.768 \times 10^{14} \tau_a(v) / f \lambda$$

where m_e is the mass of the electron, c is the speed of light, e is the electronic charge, λ is the line wavelength (in \AA) and f is the oscillator strength of the ion. *FUSE* can completely resolve the broad 1032 \AA O VI profile, however, the weaker of the OVI doublet at 1037 \AA is difficult to separate from C II* absorption at 1038 \AA . Figure 2 shows different absorption features including OVI doublet in the *FUSE* spectra of Sk-67D211 and Sk-71D45 as given in Howk *et al* [17].

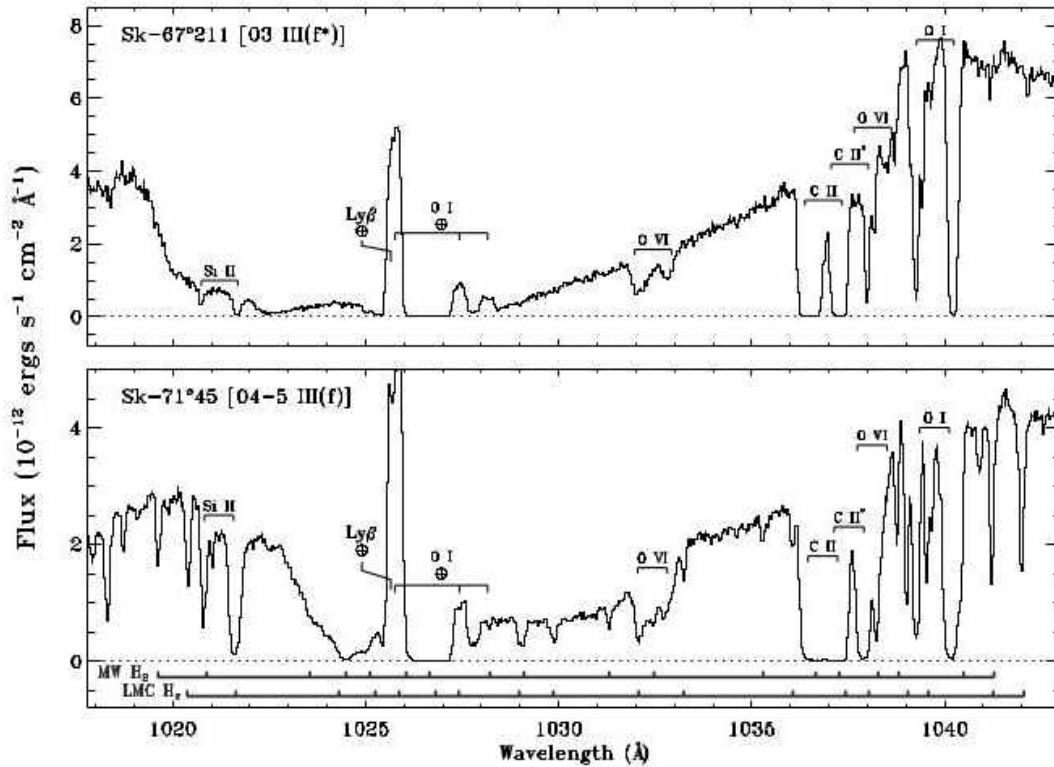


Fig 2. *FUSE* spectra of stars Sk-67D211 and Sk-71D45 showing OVI absorption features along with other Galactic absorption lines as shown by Howk *et al* [17]

3 Review of OVI absorption measurements in the Milky Way

3.1 The Local Interstellar Medium (LISM)

Oegerle *et al* [18] studied OVI 1032 Å absorption in the LISM towards 25 nearby white dwarfs (WD). They detected weak OVI absorption along all the sightlines finding a maximum column density of $1.7 \times 10^{13} \text{ cm}^{-2}$. They also found significant variation of the OVI column density over all the lines of sight and concluded that OVI has a patchy distribution in the LISM. They also found evidence of partially photospheric or circumstellar origin of OVI absorption towards hot white dwarfs. Oegerle *et al* [18] predicted that the OVI originates in evaporative interfaces between cool clouds and the hot – diffuse gas in the Local Bubble (LB). They also suggested that OVI absorption is produced over limited surfaces of clouds in the LB. They also derived a mean OVI line width of $(16 \pm 2) \text{ km s}^{-1}$ with a dispersion of 20 km s^{-1} . Savage and Lehner [19] carried out a survey of 39 WD and studied the properties of OVI in the LISM. The median value of the column density ($\log[N(\text{OVI})]$) was measured as $13.10 \text{ atoms cm}^{-2}$. Enhancement in the value of $\log [N(\text{OVI})]$ near the expected location of LB wall was found for only three WDs. OVI absorption is found to be aligned with C II for a few sightlines as expected, and for others it is displaced to positive velocities from the average velocity of C II. The evaporative flow of OVI from the interface between warm and hot gas or the cooling hot gas of the LB may be the cause of the positive velocity. The broader OVI profiles observed in this study were described as multiple component of OVI absorption and/or the evaporative outflow of conductive interface gas. OVI absorption in the LISM with column density $7 \times 10^{12} \text{ cm}^{-2}$ was detected towards REJ1043+490 [20]. In another survey Barstow *et al* [21] studied OVI absorption in the LISM using *FUSE* spectra of 80 WD. They did not find a spatial correlation between OVI and the soft X-ray background (SXR) emission. The interstellar OVI was located at or beyond the boundaries of the local cavity for few cases. They concluded that the amount of OVI bearing gas within the inner rarefied regions of the local interstellar cavity is much less than previous estimates.

3.2 Galactic disk

FUSE spectra of 150 early type stars were considered by Jenkins *et al* [22] to study the properties of O VI. They report an average number density of OVI to be $(1.7 \times 10^{-8}) \text{ cm}^{-3}$ in the Milky Way (MW) disk. Bowen *et al* [23] carried out an extensive study of OVI 1032 Å absorption line using *FUSE* observations in the Galactic disk. They considered 148 early type stars (mainly O2 – B3) with $|b| < 10^\circ$ and $|z| > 1 \text{ kpc}$ and derived OVI mid-plane density to be $(1.3 \times 10^{-8}) \text{ cm}^{-3}$. A relationship between $N(\text{OVI}) \sin |b|$ and height above the Galactic plane ($|z|$), as reported earlier for extragalactic objects, was confirmed in this study. A correlation between distance in the Galactic plane and $N(\text{OVI})$, over distances of $\sim 0.1 - 10 \text{ kpc}$ was found by Bowen *et al* [23]. They also reported another correlation between $N(\text{O VI})$ and the width of O VI absorption lines. Similarity between the velocities of the edges of OVI absorption lines and those of strong C II $\lambda 1335$ and Si III $\lambda 1206$ lines was found. In the ISM of the Galaxy, it has been noted, that OVI has higher column density towards sightlines through X-ray emitting regions. In such cases a fraction of OVI is contributed by circumstellar material or wind-blown bubble around hot young stellar associations [24].

A “coupling” between OVI profiles with the lower ionized species O I, C II, C III and Si IV has also been seen. This suggests that the structures giving rise to absorption from hot gas are multi-ionized, pointing towards the co-existence of several phases of the ISM.

Lehner *et al* [24] studied the properties of hot gas in the MW disk towards 36 sight lines as observed by *FUSE*. Most of the sight lines were within $|b| < 10^\circ$ and $|z| < 0.7 \text{ kpc}$ from the Galactic plane. Using the apparent optical depth method they found that OVI column density, $\log[N(\text{OVI})]$, is in the range $13.23 - 14.82 \text{ atom cm}^{-2}$ with an average of $14.01 \text{ atom cm}^{-2}$. They found broad OVI components that trace gas which is collisionally ionized and undergoing cooling from hot to warm/cool phase of the ISM.

3.3 Galactic halo

Savage *et al* [25] carried out the first *FUSE* study of OVI 1032 Å absorption in the Galactic halo. Out of the 11 active galactic nuclei (AGN) sightlines considered in the study, OVI absorption was detected in 10 cases. The value of $\log[N(\text{O VI})]$ in the halo using the AOD method was found in the range 13.80 to 14.64 atom cm^{-2} with a median of 14.21 atom cm^{-2} . The wide variation in the column densities found suggests irregular but widespread presence of OVI in the MW halo. OVI absorption with column density 14.38 atom cm^{-2} in the halo was measured towards quasar PG 0804+761 [26].

Howk *et al* [16] studied OVI absorption in the MW halo towards 12 early type stars in the LMC and 11 in the Small Magellanic Cloud (SMC). In the direction of the Magellanic Clouds, they found a very patchy distribution of OVI in the Galaxy. In their study they derived mean column densities $\log[N(\text{OVI})]$ using the AOD method to be 14.52 and 14.13 atom cm^{-2} towards the LMC and the SMC, respectively. Comparing OVI with Fe II distribution, they found that the OVI bearing cloud is much more extended than the cloud with Fe II in the Galaxy. As there is significant OVI column density variation over small angular scales, they suggested that the OVI bearing layer should be a composition of complicated cloud or sheet-like distribution rather than a smooth distribution of highly ionized gas. Using *FUSE* data of early type star “von Zeipel 1128”, Howk *et al* [27] derived an OVI column density of 14.49 ± 0.03 atom cm^{-2} in the Galactic halo.

FUSE spectra of a sample of 100 extra-galactic targets and two distant halo stars were considered to study OVI absorption in and around the Milky Way [28]. The work reported both weak and strong OVI absorption components at all velocities in the ranges $\sim \pm 400$ to ± 100 km s^{-1} . The average logarithmic column density of OVI is measured to be 14.33 ± 0.20 atoms cm^{-2} . In another survey, Zsargó *et al* [29] considered 22 Galactic halo stars to study OVI absorption in the halo. They found logarithmic column density in the range 13.65 to 14.56 atom cm^{-2} with an average value of 14.17 ± 0.28 atom cm^{-2} . They also confirmed the patchy distribution of OVI in the Galaxy with a mid-plane density of 1.7×10^{-8} cm^{-3} . They derived OVI scale height between 2.3 and 4 kpc. As they did not find any high velocity component in the OVI profiles, they concluded that within 2 – 5 kpc of the Galactic mid-plane, high velocity OVI is absent. From the high value of velocity dispersion (45 ± 11 kms^{-1}) Zsargó *et al* [29] suggested that the OVI profiles may be influenced by turbulence, inflow and outflow of hot gas. By comparing OVI with ArI, they found the presence of two different OVI bearing environments towards the Galactic sight lines. Indebetouw & Shull [30] studied OVI in the Galactic halo using *FUSE* spectra of 34 sight lines and derived average column density $\log[N(\text{O VI})]$ to be 14.54 atom cm^{-2} . They consider the model of smoothly distributed gas co-rotating with the Galactic disk. In another survey, the average logarithmic OVI column density was measured as 14.11 atom cm^{-2} considering the spectra of 109 Galactic stars and 30 extragalactic objects [31]. In this survey, the OVI scale height is found to be smaller than Si IV and C IV with a patchy distribution of these ions. An enhanced amount of OVI ($\sim 0.20 - 0.25$ dex) was found towards the north Galactic polar region ($b > 45^\circ$).

Considering 6 sight lines towards LMC, Sarma *et al* [32] reported a patchy distribution of OVI in the halo with mean OVI column density as 14.28 atoms cm^{-2} . The absorption profiles of these 6 sight lines are shown in Fig 3. An extensive study towards many more LMC sightlines is on-going.

4 Absorption of OVI in nearby galaxies

4.1 The LMC

Friedman *et al* [33] measured O VI absorption along the line of sight to Sk-67 D05 and found the value of $\log[N(\text{O VI})]$ in the LMC to be 13.89 ± 0.05 atoms cm^{-2} . Using *FUSE* spectra of 12 early type stars in the LMC, Howk *et al* [17] studied OVI absorption and found mean $\log[N(\text{OVI})]$ to be 14.37 cm^{-2} . Danforth *et al* [34] presented an atlas of 12 interstellar absorption lines including OVI using *FUSE* spectra of 57 LMC and 37 SMC observations. Danforth & Blair [35] studied OVI absorption towards four stars in the LMC and the value of $\log[N(\text{OVI})]$ was measured as 14.48 atoms cm^{-2} . Lehner & Howk [36] studied highly

ionized ions in the LMC using FUSE spectra of four hot stars. They measured average $\log[N(\text{OVI})]$ as 14.27 atoms cm^{-2} .

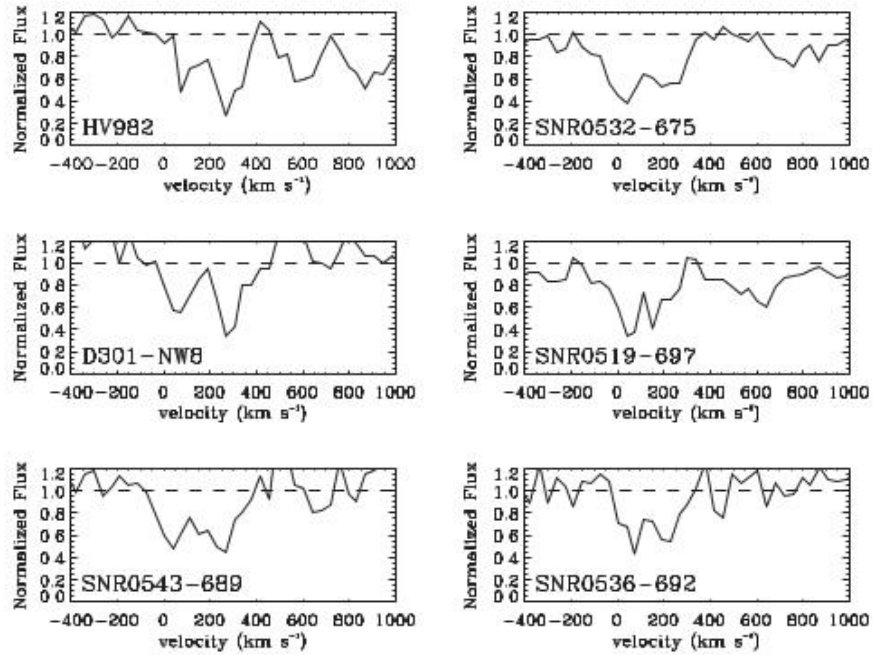


Fig 3. OVI absorption profile towards 6 sight lines in the LMC [32]

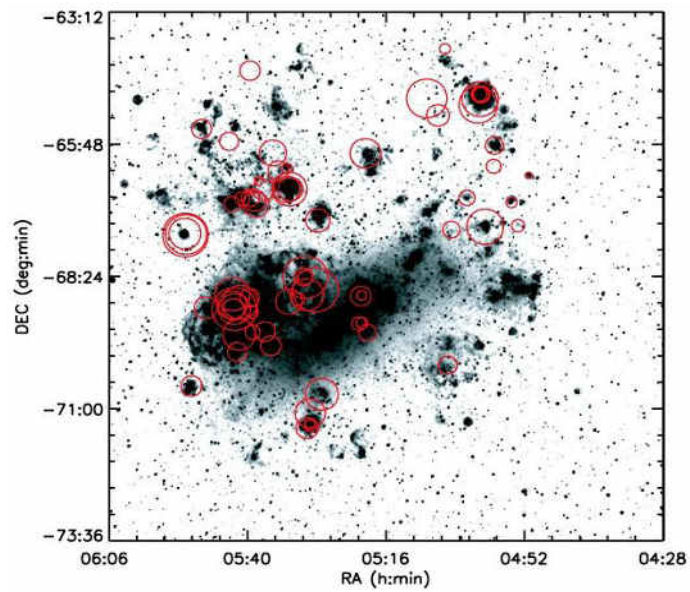


Fig 4. OVI absorption shown by circles around 70 targets in the LMC. The diameter of the circle is linearly proportional to the column density of OVI at LMC velocities. The background is an $H\alpha$ image of the LMC

In a larger survey of interstellar OVI, Pathak *et al* [37] found mean $\log[N(\text{OVI})]$ to be 14.23 atoms cm^{-2} for a sample of 70 sight lines in the LMC (Fig 4). The major results include patchiness of OVI in the ISM of the LMC. Some of the LMC sightlines have higher concentration of OVI compared to the Milky Way despite having a lower metallic content. Overall the OVI absorption did not correlate with the X-ray emission but a correlation was found for the 30 Doradus region. It is also observed that the OVI absorption decreases with the increasing distance from the star cluster R136, the major source of interstellar radiation field, pointing to a correlation with the stellar radiation field in the region. In LMC, it is also noted that Super-bubble sightlines have a higher concentration of OVI compared to non-Super-bubble sightlines.

4.2 The SMC

Hoopes *et al* [38] studied OVI absorption towards 18 OB stars and detected its presence in the SMC. They measured average column density $\log[N(\text{OVI})]$ as 14.53 atoms cm^{-2} . They found an enhanced O VI distribution near star-forming regions, especially near NGC 346 and also the southwestern complex of H II regions of the SMC. Figure 5 presents a comparison of the OVI abundances in the LMC and the SMC based on the results of Howk *et al* [16] and Hoopes *et al* [38]. Howk *et al* [16] have discussed the observed properties of interstellar OVI in the LMC with respect to the Milky Way. They have proposed a ‘corona’ model for the LMC similar to the Milky Way. They have found a patchy distribution and have not found a significant correlation with H α or X-ray emitting regions. Hoopes *et al* [38] found that the column density is correlated with position in the SMC, especially with the position from the star-forming region NGC 346. The OVI profiles in the LMC and the SMC are broader than expected from thermal broadening pointing to the fact that several components are contributing to the broadening effect.

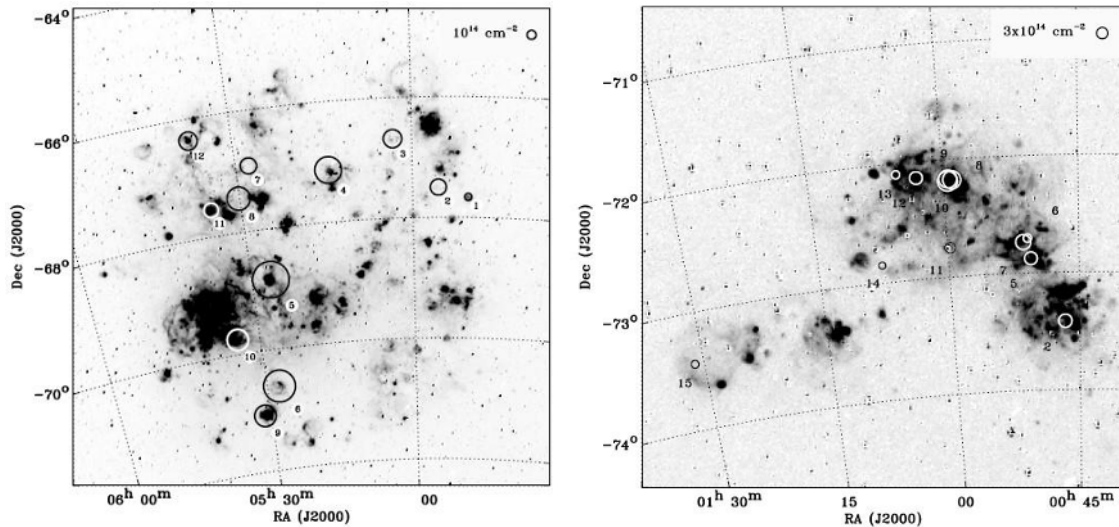


Fig 5. Comparison of the OVI distribution in the LMC (left panel adopted from Howk *et al* [16]) and the SMC (right panel adopted from Hoopes *et al* [38]). The background is an H α image of the galaxies

A summary of OVI absorption surveys discussed for the Milky Way and external galaxies are presented in Table 1. Almost every survey points to the patchy and irregular distribution of OVI. The OVI profiles have been found to be broader than predicted by the thermal broadening. This points to the fact that the broadening is only thermal but there may be several factors contributing including turbulence, outflows and inflows, etc.

Table 1. Summary of OVI absorption (values are average over the sample considered in each study)

Location	No. of stars	$\log [N(\text{OVI})]$ (atoms cm^{-2})	b (km s^{-1})	$n_{\text{O}}(\times 10^{-8}\text{cm}^{-3})$	h (kpc)	σ_{p} (dex)	References
LISM	24	13.09	23.0±5.6	-	-	-	19
	12	12.48	16±2	1.9	-	-	18
	1	12.85	10	-	-	-	20
Galactic disk							
$b > 20^{\circ}$	148	14.23	37±11	1.33±0.15	4.6±1.0	0.25	23
$b < -20^{\circ}$	148	14.23	37±11	1.34±0.17	3.2±0.8	0.25	23
Galactic halo	10	14.21	-	2.0	2.7±0.4	-	25
	91	14.38	61±15	1.7	2.3	0.25	44
Towards LMC	12	14.52	-	-	-	-	16
Towards SMC	11	14.13	-	-	-	-	16
	1	14.49	-	-	-	-	26
Other studies (MW)	102	14.33	-	-	- ^a	-	28
	22	14.17	45±11	1.7	2.3-4	-	29
	34	14.54	-	1.7	3.3	-	30
	139	14.11	-	1.64	2.6±0.5	0.233	31
	1	14.40	-	-	-	-	33
	1	13.89	-	-	-	-	33
	12	14.37	-	-	-	-	17
LMC	8	14.39	-	-	-	-	35
	4	14.48	-	-	-	-	36
	4	14.27	-	-	-	-	36
	70	14.23	-	-	-	-	37
SMC	18	14.53	-	-	-	-	38

^a $h \sim 4$ kpc for northern extragalactic sight lines.

5 Studies on OVI emission

OVI has also been observed in emission towards a limited number of sight lines in the ISM. Collision may not only result in ionization but it may also excite the oxygen ions to higher electronic states that result in subsequent emission. Otte & Dixon [39] studied OVI emission in the MW using *FUSE* spectra of 112 sight lines and found measurable O VI emission in 23 cases. The intensity of OVI emission was measured to be $1900 - 8600$ photons $\text{s}^{-1} \text{cm}^{-2} \text{sr}^{-1}$. They found a consistency in the OVI emission and absorption measurements. In another study, Shelton *et al* [40] found the OVI doublet intensity to be larger than expected for emission by the LB. They measured intensities as 2930 ± 290 and 1790 ± 260 photons $\text{s}^{-1} \text{cm}^{-2} \text{sr}^{-1}$ for 1032 and 1038 Å bands, respectively. They suggested that the observed intensity must arise in the Galactic thick disk or lower halo. OVI flux estimation from emission spectra is complicated as self-absorption and resonant scattering complicates the OVI emission measurements [40]. Dixon & Sankrit [41] studying the OVI emission suggested large-scale structure of the OVI bearing gas in the quadrant of the sky centered on

the Magellanic Clouds. OVI emission in the interface region of Magellanic System was also detected by them. The lowest intensity of OVI emission in the MW was measured to be 1600 ± 300 photons $s^{-1} \text{ cm}^{-2} \text{ sr}^{-1}$ (for the 1032 Å feature) and 800 ± 300 photons $s^{-1} \text{ cm}^{-2} \text{ sr}^{-1}$ (for the 1038 Å feature) [42]. The observed OVI emission is suggested to be produced in the Galactic halo by hot gas ejected by supernovae in the spiral arms. Using FUSE data, Sankrit & Dixon [43] studied WD KPD 0005 + 5106. They measured the density of the nebula to be $\sim 10 \text{ cm}^{-3}$. Based on the synthetic spectrum of WD and photoionization models for the nebular emission, they inferred the existence of a circumstellar shell between the star and the OVI emitting nebula.

6 Distribution of OVI

A modest excess of OVI is seen in the LISM compared to the more distant interstellar regions [18]. OVI absorption arises over limited region on the surfaces of clouds within the local bubble. Magnetic field may control the conduction over the surface of each cloud [18]. The properties of OVI absorption are found to be consistent with the results of the theory of conductive interfaces for its origin [19].

In the disk of the Milky Way, OVI is present almost towards every direction but the distribution is not uniform. OVI volume density decreases with the height above the plane of the Galaxy. Conventionally, it has been assumed that the gas distribution is smooth and decreases exponentially as $n|z| = n_0 \exp(-|z|/h)$, where h is the scale height, n_0 is the mid-plane density and z is the height above the plane of the Galaxy. This simple exponential model of gas distribution exhibits a large dispersion. Addition of a new parameter ‘‘patchiness’’ or degree of irregularity to the simple model can very well describe the gas distribution [23, 31, 44]. The OVI scale height of (2.7 ± 0.4) kpc have been obtained by Savage *et al* [25]. Bowen *et al* [23] derived O VI a scale height of 4.6 kpc and 3.2 kpc, respectively for sight lines in the southern and northern Galactic hemisphere.

The OVI absorbing clouds are not smoothly distributed in the ISM rather they are of different sizes with varying concentration of OVI. In the halo, OVI may reside in hot clouds ($T \sim 3 \times 10^5 \text{ K}$) or in the interface of the hot ($T \geq 10^6 \text{ K}$) and cool ($T < 10^5 \text{ K}$) gas of the ISM [16].

The OVI column density and distance over which the measurements are made have been found to be correlated. This means that the sight lines tracing more absorbing clouds show a higher concentration of OVI, which further suggests that OVI generation is an interstellar phenomenon. Beyond a few hundred parsec, a discontinuity in $N(\text{OVI})$ arises because of the contribution from the LB [23].

The distribution of OVI in the northern and southern Galactic hemispheres do not correlate. Savage *et al* [25] noticed a clear difference in OVI column density towards stars in the northern and southern Galactic hemispheres. For the north Galactic polar region with $(45^\circ < b < 90^\circ)$ there is an excess of 0.20 to 0.30 dex in the average value of $\{\log[N(\text{OVI}) \times \sin|b|]\}$ compared to the lower north latitude direction and the southern Galactic hemisphere.

The OVI column densities also show significant variation over small angular scales. Howk *et al* [16] studied the variation in OVI column density observed towards the LMC and the SMC. The average column density difference in the MW halo towards stars in the LMC over angular scales of 0.5° to 5.0° is about 0.21 dex. The OVI column density difference over angular scales of 0.05° to 3.3° towards the SMC is found to be about 0.20 dex [16]. Savage *et al* [44] have estimated this variation on a much larger angular scale. Zsargó *et al* [29] also found significant small scale variations in the OVI column density for closely aligned extragalactic objects. Sarma *et al* [45] found OVI column density variation at much smaller angular scales. The smallest scale for which O VI column density variation has been estimated is $\sim 1^\circ.44$ ($\sim 0.28 \text{ pc}$). The small scale column density variations may be a local phenomenon or it may extend to the entire halo. An extensive study is desired to get further insights.

7 Line width of the OVI profile

Significant variations have been seen in the line width of the OVI profile in the ISM of the MW and that of external galaxies. It is difficult to understand the deviation (mostly increasing) of the line width estimated by the CIE and the temperature traced by OVI. The profiles of OVI have been compared to the profiles of Fe II (λ 1125.45). It has been observed that the OVI profiles are significantly broader. This particularly exhibits the dominance of the intermediate velocity and high velocity clouds in case of OVI. This also points to the complex kinematics of the hot gas (traced by highly ionized atoms; OVI in this case) compared to relatively cooler gas (traced by low ions; Fe II in this case).

A correlation between OVI column density and Doppler parameter is seen for the LISM, the Galactic disk, the Galactic halo and beyond [44, 46]. This correlation could be the result of the superposition of contributions to column density and Doppler parameter from multiple interfaces of the gas displaced in velocity [19]. The progressive increase in the average line width from the LISM to the Galactic halo suggests an increase in the number of the OVI bearing clouds [29].

8 Summary

OVI being an important tracer of the warm-hot phase of the ISM, extensive studies have been carried out using space telescope data on UV absorption spectra of Galactic and extragalactic objects. *FUSE* has contributed significantly to the study of OVI through its high resolution spectroscopic instrument. The *FUSE* data have improved our understanding of the formation and distribution of OVI in the ISM of the Milky Way and in nearby galaxies. Here we have discussed different studies of OVI absorption and emission in the Milky Way and in the nearby galaxies. The main features of OVI distribution may be summarized as follows:

1. From the OVI absorption in the MW, it is understood that it originates from conductive interfaces between cool clouds and a much hotter medium [47] or in turbulent mixing layers on the surfaces of clouds that are moving with respect to their surroundings [48].
2. An enhanced distribution of OVI is seen in the north Galactic polar region ($b > 45^\circ$). The average OVI column density value increases from LISM to the Galactic halo. Column density is in the range 12.48 – 13.09 atom cm^{-2} in the LISM, 14.01 – 14.23 atom cm^{-2} in the disk and 14.11 – 14.54 atom cm^{-2} in the halo of the Galaxy.
3. The mean OVI column density in the LMC is comparable to the Galactic halo. OVI column density in the SMC is higher than the LMC or the Galactic halo. This is surprising as the SMC has a lower metallicity compared to the LMC and the Milky Way.
4. The distribution of OVI throughout the Milky Way and in the ISM of external galaxies is patchy. The level of irregularity which is measured by the parameter “patchiness” to properly describe the distribution of the OVI bearing gas ranges from 0.233 – 0.28.
5. In several of the OVI absorption studies, the Doppler width b for OVI profiles is found to be much larger than the thermal broadening for a gas at $T \sim 3 \times 10^5$ K. This suggests that the OVI ion exists in multiple environments dominated by inflow, outflow and turbulence. The average line width increases from the LISM to the Galactic halo which suggests an increasing number of OVI bearing clouds.

Acknowledgements

AP acknowledges financial support from SERB – DST FAST TRACK and DST – JSPS grants and associateship of the Inter-University Centre for Astronomy and Astrophysics, Pune.

References

1. Spitzer L(Jr), *ApJ*, 124(1956)20-34.
2. Morton D C, *ApJS*, 77(1991)119-202.
3. Sutherland R S, Dopita M A, *ApJS*, 88(1988)253-327.
4. Jenkins E B, Meloy D A, *ApJ*, 193(1974)L121-L125.
5. York D G, *ApJ*, 193(1974)L127-L131.
6. Jenkins E B, *ApJ*, 219(1978)845-860.
7. Jenkins E B, *ApJ*, 220(1978)107-123.
8. Davidsen A F, *Science*, 259(1993)327-334.
9. Hurwitz M, Appenzeller I, Barnstedt J, Bowyer S, Van Dyke Dixon W, Grewing M, Kappelmann N, Krämer G, Krautter J, Mandel H, *ApJ*, 500(1998)L61. doi.org/10.1086/311396
10. Moos H W, Cash W C, Cowie L L, Davidsen A F, Dupree A K, Feldman P D, Friedman S D, Green J C, Green R F, Gry C, Hutchings J B, Jenkins E B, Linsky J L, Malina R F, Michalitsianos A G, Savage B D, Shull J M, Siegmund O H W, Snow T P, Sonneborn G, Vidal-Madjar A, Willis A J, Woodgate B E, York D G, Ake T B, Andersson B-G, Andrews J P, Barkhouser R H, Bianchi L, Blair W P, Brownsberger K R, Cha A N, Chayer P, Conard S J, Fullerton A W, Gaines G A, Grange R, Gummin M A, Hebrard G, Kriss G A, Kruk J W, Mark D, McCarthy D K, Morbey C L, Murowinski R, Murphy E M, Oegerle W R, Ohl R G, Oliveira C, Osterman S N, Sahnou D J, Saisse M, Sembach K R, Weaver H A, Welsh B Y, Wilkinson E, Zheng W, *ApJ*, 538(2000)L1; doi.org/10.1086/312795
11. Sahnou D S, Moos H W, Ake T B, Andersen J, Andersson B-G, Andre M, Artis D, Berman A F, Blair W P, Brownsberger K R, Calvani H M, Chayer P, Conard S J, Feldman P D, Friedman S D, Fullerton A W, Gaines G A, Gawne W C, Green J C, Gummin M A, Jennings T B, Joyce J B, Kaiser M E, Kruk J W, Lindler D J, Massa D, Murphy E M, Oegerle W R, Ohl R G, Roberts B A, Romelfanger M L, Roth K C, Sankrit R, Sembach K R, Shelton R L, Siegmund O H W, Silva C J, Sonneborn G, Vaclavik S R, Weaver H A, Wilkinson E, *ApJ*, 538(2000)L7. doi.org/10.1086/312794.
12. Murthy J, Sahnou D J, *ApJ*, 615(2004)315. doi.org/10.1086/424441
13. Dixon W V, Sahnou D J, Barrett P E, Civeit T, Dupuis J, Fullerton A W, Godard B, Hsu J.-C, Kaiser M E, Kruk J W, Lacour S, Lindler D J, Massa D, Robinson R D, Romelfanger M L, Sonnentrucker P, *PASP*, 119(2007)527-555.
14. Savage B D, Sembach K R, *ApJ*, 379(1991)245-259.
15. Sembach K R, Savage B D, *ApJS*, 83(1992)147-201.
16. Howk J C, Savage B D, Sembach K R, Hoopes C G, *ApJ*, 572(2002)264; doi.org/10.1086/340231
17. Howk J C, Sembach K R, Savage B D, Massa D, Friedman S D, Fullerton A W, *ApJ*, 569(2002)214; doi.org/10.1086/339322.
19. Savage B D, Lehner N, *ApJS*, 162(2006)134-160.
20. Welsh B Y, Sallmen S, Lallement R, *A & A*, 414(2004)261-274.
21. Barstow M A, Boyce D D, Welsh B Y, Lallement R, Barstow J K, Forbes A E, Preval S, *ApJ*, 723(2010)1762-1786.
22. Jenkins E B, Bowen D V, Sembach K R, in *Galactic and Intergalactic Space*, (eds) R Ferlet, M Lemoine, J.-M. Desert, B Raban, (Paris: Frontier Group), 2001, 99.
23. Bowen D, Jenkins E B, Tripp T M, Sembach K R, Savage B D, Moos H W, Oegerle W R, Friedman S D, Gry C, Kruk J W, Murphy E, Sankrit R, Shull J M, Sonneborn G, York D G, *ApJS*, 176(2008)59; doi.org/10.1086/524773
24. Lehner N, Zech W F, Howk J C, Savage B D, *ApJ*, 727(2011)46; doi.org/10.1088/0004-637X/727/1/46.
25. Savage B D, Sembach K R, Jenkins E B, Shull J M, York D G, Sonneborn G, Moos H W, Friedman S D, Green J C, Oegerle W R, Blair W P, Kruk J W, Murphy E M, *ApJ*, 538(2000)L27; doi.org/10.1086/312792
26. Richer P, Savage B D, Wakker B P, Sembach K R, Kalberla P M W, *ApJ*, 549(2001)281-292; doi.org/10.1086/319070

27. Howk C J, Sembach K R, Savage B D, *ApJ*, 586(2003)249; doi.org/10.1086/346262
28. Wakker B P, Savage B D, Sembach K R, Richter P, Meade M, Jenkins E B, Shull J M, Ake T B, Blair W P, Dixon W V, Friedman S D, Green J C, Green R F, Kru J W, Moos H W, Murph E M, Oegerle W R, Sahnou D J, Sonneborn G, Wilkinson E, York D G, *ApJS*, 146(2003)1-123.
29. Zsargó J, Sembach K R, Howk J C, Savage B D, *ApJ*, 586(2003)1019. doi.org/10.1086/367766.
30. Indebetouw R, Shull M J, *ApJ*, 607(2004)309. doi.org/10.1086/383465
31. Savage B D, Wakker, B P, *ApJ*, 702(2009)1472. doi.org/10.1088/0004-637X/702/2/1472.
32. Sarma R, Pathak A, Pradhan A C, Murthy J, Sarma J K, *Adv Sp Res*, 5(2014)963-966.
33. Friedman S D, Howk J C, Andersson B-G, Sembach K R, Ake T B, Roth K, Sahnou D J, Savage B D, York D G, Sonneborn G, Vidal-Madjar A, Wilkinson E, *ApJ*, 538(2000)L39; doi.org/10.1086/312800
34. Danforth C W, Howk J C, Fullerton A W, Blair W P, Sembach K R, *ApJS*, 139(2002)81-189; doi.org/10.1086/338239
35. Danforth C W, Blair W P, *ApJ*, (646)(2006)205. doi.org/10.1086/504706
36. Lehner N, Howk C J, *MNRAS*, 377(2007)687-704.
37. Pathak A, Pradhan A C, Sujatha N V, Murthy J, *MNRAS*, 412(2011)1105-1122.
38. Hoopes C G, Sembach K R, Howk J C, Savage B D, Fullerton A W, *ApJ*, 569(2002)233. doi.org/10.1086/339323
39. Otte B, Dixon W V D, *ApJ*, 647(2006)312-327.
40. Shelton R L, Kruk J W, Murphy E M, Andersson B G, Blair W P, Dixon W V, Edelstein J, Fullerton A W, Gry C, Howk J C, Jenkins E B, Linsky J L, Moos H W, Oegerle W R, Oey M S, Roth K C, Sahnou D J, Sankrit R, Savage B D, Sembach K R, Shull J M, Siegmund O H W, Vidal-Madjar A, Welsh B Y, York D G, *ApJ*, 560(2001)730. dx.doi.org/10.1086/322478
41. Dixon D W, Sankrit R, *AIP Conf Proc*, 1135(2009)102-106.
42. Otte B, Dixon D W, Sankrit R, *ApJ*, 586(2003)L53. doi.org/10.1086/374731
43. Sankrit R, Dixon D W, *ApJ*, 701(2009)481. doi.org/10.1088/0004-637X/701/1/481
44. Savage B D, Sembach K R, Wakker B P, Richter P, Meade M, Jenkins E B, Shull J M, Moos H W, Sonneborn G, *ApJS*, 146(2003)125-164..
45. Sarma R, Pathak A, Murthy J, Sarma J K, *MNAS*, (2015) submitted.
46. Heckman T M, Norman C A, Strickland D K, Sembach K R, *ApJ*, 577(2002) 691. doi.org/10.1086/342232
47. Cowie L L, Jenkins E B, Songaila A, York D G, *ApJ*, 232(1979)467-472.
48. Slavin J D, Shull J M, Begelman M C, *ApJ*, 407(1993)83-99.

[Received : 9.6.2015; accepted : 21.6.2015]